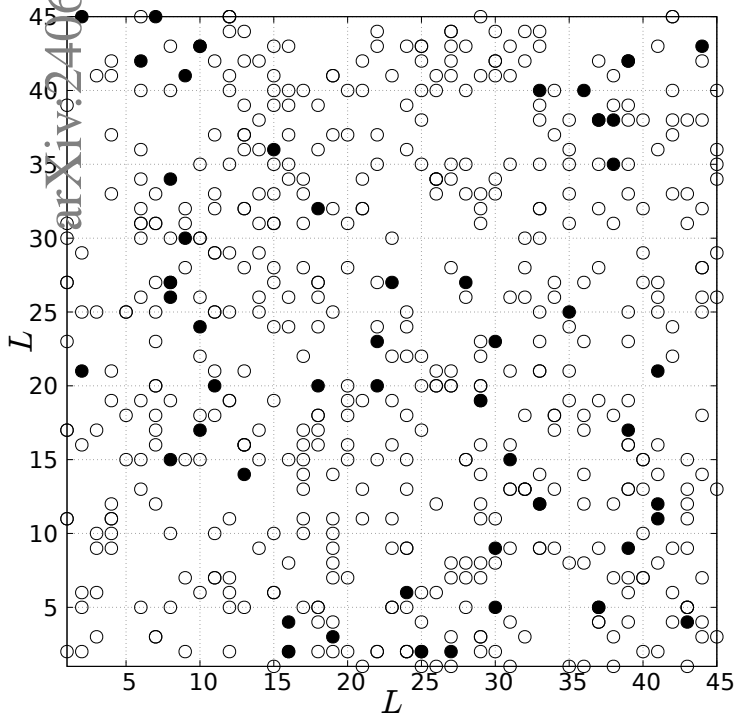


Graphical Abstract

Emergence of social hierarchies in a society with two competitive classes

Marc Sadurní, Josep Perelló, Miquel Montero



Highlights

Emergence of social hierarchies in a society with two competitive classes

Marc Sadurní, Josep Perelló, Miquel Montero

- An extended Bonabeau model develops social hierarchies and clear leadership.
- Dynamics driven by agent reputation interactions is independent of system size.
- A behavioural transition from egalitarian to hierarchical society is found.
- Scaling laws are provided to explain the role of the variables of the model.

Emergence of social hierarchies in a society with two competitive classes

Marc Sadurní^{a,b,*}, Josep Perelló^{a,b,*} and Miquel Montero^{a,b,*}

^aDepartament de Física de la Matèria Condensada, Universitat de Barcelona, Martí i Franquès, 1, Barcelona, 08028, Catalonia, Spain

^bUniversitat de Barcelona Institute of Complex Systems, Martí i Franquès, 1, Barcelona, 08028, Catalonia, Spain

ARTICLE INFO

Keywords:

Complex Systems
Spatial inequalities
Social hierarchies
Agent-based models
Stochastic processes

ABSTRACT

Agent-based models describing social interactions among individuals can help to better understand emerging macroscopic patterns in societies. One of the topics which is worth tackling is the formation of different kinds of hierarchies that emerge in social spaces such as cities. Here we propose a Bonabeau-like model by adding a second class of agents. The fundamental particularity of our model is that only a pairwise interaction between agents of the opposite class is allowed. Agent fitness can thus only change by competition among the two classes, while the total fitness in the society remains constant. The main result is that for a broad range of values of the model parameters, the fitness of the agents of each class show a decay in time except for one or very few agents which capture almost all the fitness in the society. Numerical simulations also reveal a singular shift from egalitarian to hierarchical society for each class. This behaviour depends on the control parameter η , playing the role of the inverse of the temperature of the system. Results are invariant with regard to the system size, contingent solely on the quantity of agents within each class. Finally, a couple of scaling laws are provided thus showing a data collapse from different model parameters and they follow a shape which can be related to the presence of a phase transition in the model.


1. Introduction


During last decades, computational science has been playing a crucial role in the study of numerous compelling domains. Within this broad field, agent-based modelling (ABM) simulates behaviour and interactions of heterogeneous units to find regularities and macroscopic properties that can help to better understand real-world phenomena [1]. In Physics, agent-based modelling has been widely explored in the context of molecular dynamics [2, 3] with the extensive use of Monte Carlo simulations [4]. Agent-based modelling has also been implemented in the contexts of social physics [5] and computational social science (CSS) [6]. The main aim in this context is to understand human behaviour within a society in terms of the interaction among their individuals. The basic constituents are not particles but humans interacting with a small number of partners compared to the total size of the system [7]. As a result, statistical physics has been offering valuable insights into various socioeconomic systems. It has contributed to the analysis of macroscopic natural phenomena and it has facilitated the comprehension of large-scale consistencies emerging from the interactions among individual entities [7]. These interactions often produce transitions from disorder to order and the system follows scaling laws that unveil certain universal properties [7].

Hierarchy formation has been a stimulating complex emergence phenomenon in social sciences [8–11]. In 1951, Landau emphasized that intrinsic characteristics of individuals, such as weight and aggressiveness, proved to be insufficient in explaining the emergence of observed hierarchies and pointed that one shall be carefully looking at the interactions among individuals [9]. The hierarchy of social organization is an omnipresent property of animal and human aggregations. The emergence of class structures can be observed in many kinds of societies such as insects [12], fishes [13, 14], birds [15], mammals [16], and of course in humans groups [17, 18]. If one particularly consider human societies, then cities become a relevant context in which social inequities organically emerge [19–21].

During the 1990s, Bonabeau et al. [22] proposed a computationally-based model motivated by the empirical observations where dominance relationships seem to be established by the result of fights between individuals. The

*Corresponding authors

 marc.sadurni@ub.edu (M. Sadurní); josep.perello@ub.edu (J. Perelló); miquel.montero@ub.edu (M. Montero)

 <https://www.ubics.net/sadurni-parera-marc/> (M. Sadurní); <https://www.ubics.net/perello-palou-josep/> (J.

Perelló); <https://www.ubics.net/montero-torralbo-miquel/> (M. Montero)

ORCID(s): 0000-0002-9870-5513 (M. Sadurní); 0000-0001-8533-6539 (J. Perelló); 0000-0002-3221-1211 (M. Montero)

model relies on the existence of a feedback mechanism [23] where individuals who have won more fights are more likely to win future fights. Through a simple algorithm in which individuals move on a square grid, the model thus shows that self-organized hierarchies can emerge spontaneously from an egalitarian society. Many modifications and extensions have been done to make the model more realistic. The most renowned modification was proposed by Stauffer [24] which involves the adjustment of a parameter within the feedback mechanism of the system. Reference [25] found that the egalitarian solution of the Stauffer version is always stable, while a two-level stable solution (a hierarchical profile) emerges at a critical parameter value via a saddle-node bifurcation. Further improvements of the model are reported in several references [25–29]. Besides these modifications that aim to enhance realism, there are also articles attempting to simplify the Bonabeau model [30–32] or even to calibrate the model with real-world data from animals and humans [33].

We here introduce a novel approach to the Bonabeau model. We explore a new version of the Bonabeau model where an additional class is introduced in the society. The interactions between individuals of the same class are forbidden, only interactions among individuals of different class are kept. Employing a discrete scheme, we create a mean field approximation that enables us to characterize the intricacies of hierarchical pattern formation. The model can represent the interaction of two distinct groups that might be living or sharing same physical space. The minimalist interacting agent model accounts for the development of social diversity which might be taking place in social contexts such as cities. Interactions might be between two ethnic or cultural populations, between migrants or tourists and native residents. It can also be representing interactions between two polarized income groups, or even between two competing criminal gangs [19–21, 34].

The paper is organized as follows. In Section 2, we introduce an extension of the original Bonabeau model which incorporates a second class into the society and describes the interaction rules between the two classes. In Section 3, results via computer simulations are reported. In particular, we describe the time-evolution of key macroscopic values of the model and compute the Gini coefficient under different conditions. In Section 4, we explore the formation of hierarchical structures in the long run. Two scaling laws are suggested in Section 5. Finally, we conclude in Section 6, where we summarize key results. We there also include general discussions about the link of the model with real-world phenomena, discuss the limitations of the model and point to possible future work.

2. The Bonabeau model with two classes of agents

The Bonabeau model [22] describes the evolution with time t of the so-called fitness functions from N agents that interact within a society. The agents move following random walks on a two-dimensional square lattice $L \times L$. The fitness of an agent i is continuous, positive, and changes at every timestep Δt due to pairwise interactions of agents sharing the same location in the lattice. The Bonabeau model understands interactions as a competition between agents. If agent i and agent j interacts, there are two possibilities: (1) agent i wins and therefore the fitness increases by a constant value δ^+ or (2) agent i loses and therefore the fitness decreases by a constant value δ^- . The same rule applies for agent j and its fitness. The outcome of the interaction is assumed to be probabilistic: the larger the value of the fitness, the higher probability of winning the encounter by the agent i . The Bonabeau model [22] assumes for simplicity $\delta^+ = \delta^- = 1$, so that the fitness is proportional to the number of wins minus the number of losses. Results of the Bonabeau model show a transition from egalitarian to hierarchical state as the density $\rho = N/L^2$ increases.

In contrast to the original Bonabeau model, our approach assumes the existence of two distinct classes within a society. Agents exclusively compete with agents belonging to the opposing class. We thus designate by $F_i^A(t)$ the fitness of the N_A agents belonging to a first class A (where $i \in \{1, \dots, N_A\}$). And we then designate by $F_j^B(t)$ the fitness of the N_B agents belonging to a second class B (where $j \in \{1, \dots, N_B\}$). At time t , agent i with fitness $F_i^A(t)$ interacts with agent j with fitness $F_j^B(t)$ if they both occupy the same location. After the interaction, they exchange a certain amount of fitness proportional to parameter $0 < x < 1$. If agent i wins, the fitnesses change during time step Δt in the following way:

$$\begin{aligned} F_i^A(t + \Delta t) &= F_i^A(t) + xF_j^B(t), \\ F_j^B(t + \Delta t) &= F_j^B(t) - xF_j^B(t), \end{aligned} \tag{1}$$

while if agent i loses, the fitnesses exchange read:

$$\begin{aligned} F_i^A(t + \Delta t) &= F_i^A(t) - xF_i^A(t), \\ F_j^B(t + \Delta t) &= F_j^B(t) + xF_i^A(t). \end{aligned} \quad (2)$$

Unlike the original Bonabeau model, here we do not include a relaxation term [22].

Winning or losing depends on probability $P_{ij}(t)$. Following the definition from the original Bonabeau model [22], winning probability of agent i over agent j reads:

$$P_{ij}(t) = \frac{1}{1 + \exp \left[\eta \left(\hat{F}_j^B(t) - \hat{F}_i^A(t) \right) \right]}, \quad (3)$$

where we have defined the normalized fitness as:

$$\begin{aligned} \hat{F}_i^A(t) &= \frac{F_i^A(t) - F_{\min}^A(t)}{F_{\max}^A(t) - F_{\min}^A(t)}, \\ \hat{F}_j^B(t) &= \frac{F_j^B(t) - F_{\min}^B(t)}{F_{\max}^B(t) - F_{\min}^B(t)}, \end{aligned} \quad (4)$$

where $F_{\min}^A(t) \equiv \min\{F_i^A(t)\}$ and $F_{\min}^B(t) \equiv \min\{F_j^B(t)\}$ are the smallest non-normalized fitness values for each class, and $F_{\max}^A(t) = \max\{F_i^A(t)\}$ and $F_{\max}^B(t) = \max\{F_j^B(t)\}$ are the highest non-normalized fitness values for each class. Two alternative ways of normalizing fitness are presented in *Appendix A*. They both show the same qualitative behaviour.

Equation (3) also incorporates the parameter $\eta > 0$ which regulates the intensity of the interactions. In physical terms, η can be interpreted as the inverse of the temperature of the system [22]. The winning probability $P_{ij}(t)$ depends on the normalized fitness difference of agents j and i . The larger the normalized fitness of the agent i , the higher the probability of winning. Note that if $\hat{F}_i^A(t) \gg \hat{F}_j^B(t)$, $P_{ij}(t)$ tends to 1. If $\hat{F}_i^A(t) \ll \hat{F}_j^B(t)$, $P_{ij}(t)$ tends to 0.

We can also define the overall fitness for the entire society as:

$$\phi = \sum_{i=1}^{N_A} F_i^A(t) + \sum_{j=1}^{N_B} F_j^B(t) = F_{\text{tot}}^A(t) + F_{\text{tot}}^B(t). \quad (5)$$

The total fitness ϕ is constant (independent of time t) because the interaction between two agents always preserve the total fitness.

All agents of both classes are moving on a $L \times L$ square lattice following a random walk (for one static class, the results qualitatively do also not vary). In order to reproduce the time that a jump happens and also to determine which agent class moves, a residence time algorithm (the Gillespie algorithm) has been implemented [35]. Agents are bosons, i.e., there can be many agents in the same site. The interaction takes place when the moving agent goes to a site that is occupied by one or more agents of the opposite class. If there are multiple agents from the other class, one single agent is randomly chosen to interact with. A flux diagram of the code is shown in Figure 1. More details of the simulation techniques are reported in *Appendix B* and the computer code is available in GitHub [36].

3. Fitness temporal evolution

Initially (at time $t = 0$), all agents are randomly distributed over the lattice. See in Figure 2 one initial setting to exemplify agents' distribution in a $L \times L$ square lattice. Their fitness value is initially set to $F_i^A(0) = F_j^B(0) = \phi / (N_A + N_B)$: the so-called egalitarian regime. As defined, the results are entirely invariant to the total fitness of the whole society. For clarity, we set ϕ to 1 000 arbitrary units for all simulations presented in this section.

3.1. Parameter dependence

We first conduct a coarse-grained analysis of the temporal evolution of agents' fitness to examine its reliance on all model parameters. Figure 3 shows the time evolution of the fitness of all agents from the class B ($N_B = 50$). We

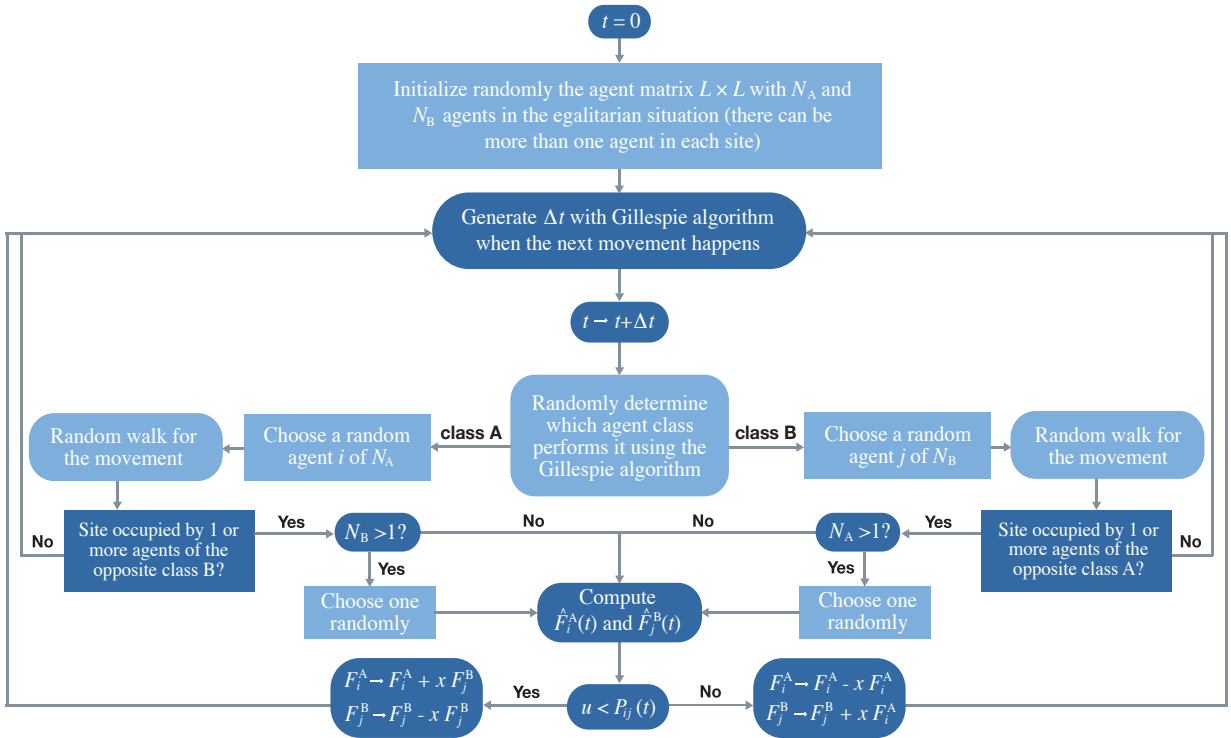


Figure 1: Flux code diagram of computer simulations. Flux code diagram of the Monte Carlo simulations with the Gillespie algorithm implemented, where $u \sim U(0, 1)$ is a uniform random number between 0 and 1. A detailed description can be found in *Appendix B*.

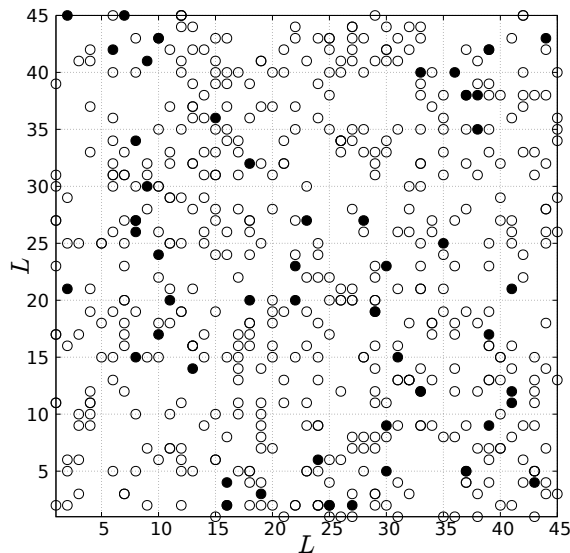


Figure 2: Initial spatial distribution of agents in a regular square lattice. Initial random positions of both classes of agents with $N_A = 500$ (empty circles) and $N_B = 50$ (filled circles) for $L = 45$. There can be more than one agent in each site.

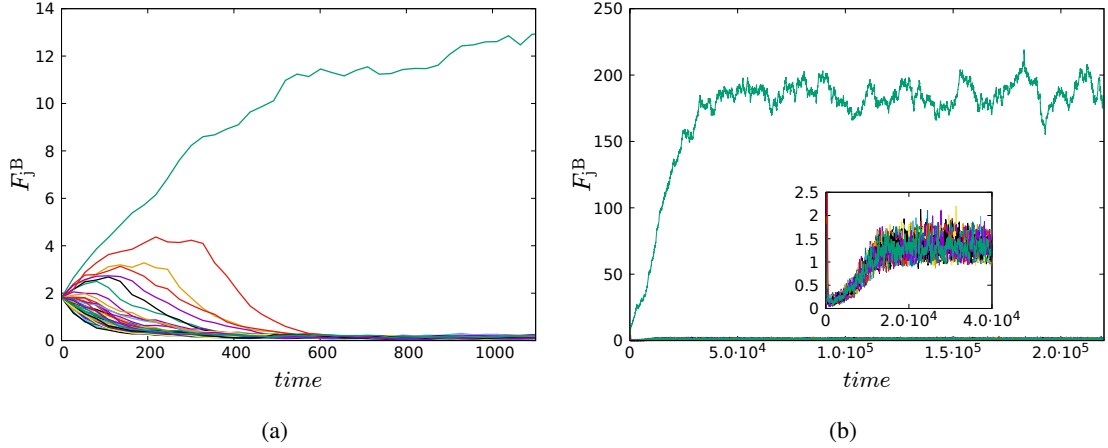


Figure 3: Temporal evolution of the fitnesses of class B. Time evolution of all F_j^B for $N_A = 500$ and $N_B = 50$ individuals, $\eta = 5$ and $x = 0.01$, randomly simulated on a $L \times L$ lattice ($L = 25$). (a) The first 1100 time steps. (b) Larger time window to observe the transient and stationary fluctuations of the leader while the inset shows the behaviour of the other agents of the class.

there fix a particular set of values of the parameters and then represent the first 1100 steps in Figure 3 (a) to see how a leader emerges in this specific model setup. The same applies to the class A. Figure 3 (b) shows how the leader fluctuates around a stationary value for large enough times (the stationary regime). The inset of Figure 3 (b) illustrates the transient behaviour for the rest of agents (those keeping just a small portion of the total fitness). The phenomena shown in the inset arises when a single leader emerges in the opposite class, triggering subsequent fitness exchanges among the rest of the agents until a stable regime is reached.

After repeating the simulations while only modifying the system size L , we get the trajectories showed in *Appendix C*. We can observe that, regardless of the value of L , one agent emerges as a leader for the same parameters in Figure 3. We will later see that the leader emergence might not be always the case as this will depend on the parameters choice. Figure 4 closely examines both $F_{\max}^A(t)$ and $F_{\max}^B(t)$ in the stationary regime. We there explore several system sizes L . The time required to reach the stationary regime for maximum fitness is longer for larger values of L . Indeed, we observe that the time required to reach the stationary regime for maximum fitness increases in a polynomial manner with respect to the system size L as described in *Appendix C*. Except for illustration purposes, we keep the system size constant setting the $L \times L$ square lattice to a constant value $L = 25$. This relatively small value leads to a quicker attainment of the stationary regime and it reduces CPU time.

We now compare the time evolution of the two classes with N_A and N_B agents in Figure 5. Figure 5 (b) shows that after 20000 Gillespie time units, the class B ($N_B \ll N_A$) is dominated by a single agent. In contrast, Figure 5 (a) shows that there are still multiple agents sharing an equal amount of fitness in the class A. No marked leader has yet emerged. Therefore, inequalities emerge more rapidly in the class with the smallest size.

We can also vary the number of agents in the system (N_A and N_B). In Figure 6 we consider the maximum fitness values of each class, $F_{\max}^A(t)$ and $F_{\max}^B(t)$, and their total fitness $F_{\text{tot}}^A(t)$ and $F_{\text{tot}}^B(t)$ for several combinations of the number of agents. In particular, in Figure 6 (c) compared to Figure 6 (a), the fraction $N_A/N_B = 10$ is kept constant by doubling N_A and N_B . On the other hand, in Figure 6 (b) the total number of agents $N_T = N_A + N_B = 550$ is maintained constant in respect to Figure 6 (a) while the fraction $N_A/N_B = 1.75$ is reduced, making classes more equal in size. Ultimately, the number of agents illustrated in Figure 6 (d) can be determined from Figure 6 (b) by keeping constant the fraction $N_A/N_B = 1.75$ and doubling N_A and N_B . Analysing in detail the four Figures, several conclusions can be drawn. In the first case, while maintaining the fraction constant, and duplicating N_T , results in impact on $F_{\text{tot}}^A(t)$ and $F_{\text{tot}}^B(t)$, and also notable reductions in $F_{\max}^A(t)$ and $F_{\max}^B(t)$ as N_T increases. Conversely, when the total number of agents N_T remains the same but the ratio N_A/N_B changes, a quite different behaviour is observed. The stationary regime for the maximum fitnesses remain invariable, but there is a considerable alteration in the distribution of fitness between classes. Indeed, the emergence of a leader is closely tied to the distance that separates the values of $F_{\max}^A(t)$ and $F_{\text{tot}}^A(t)$ and the values of $F_{\max}^B(t)$ and $F_{\text{tot}}^B(t)$. An increased gap between these two lines corresponds to a reduced inequality among

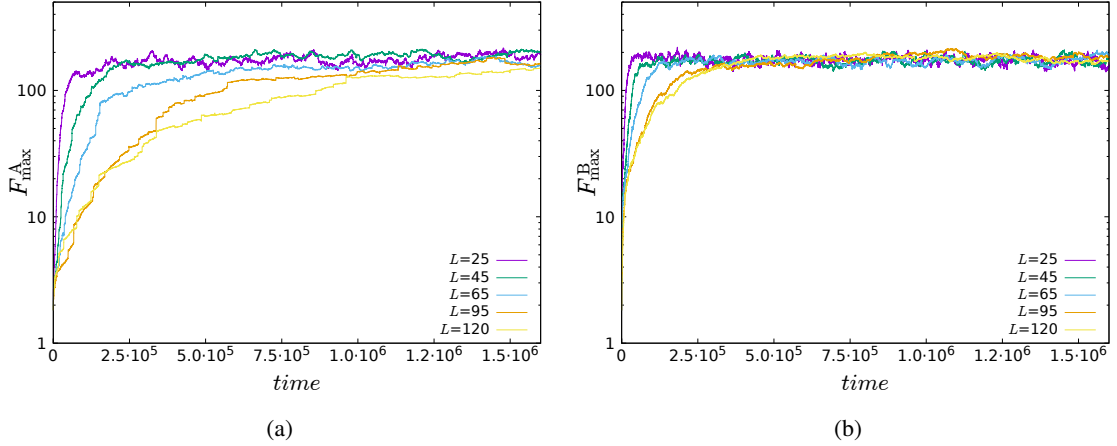


Figure 4: Maximum fitness temporal evolution of the two classes for several systems sizes. Time evolution of the maximum fitness for $N_A = 500$ and $N_B = 50$ agents, $\eta = 5$ and $x = 0.01$, randomly simulated on several $L \times L$ square lattice sizes (largest to smallest ascending). (a) $F_{\max}^A(t)$ and (b) $F_{\max}^B(t)$. The vertical axis is in log scale.

agents in a class, while a narrower gap signifies greater inequality among agents. Hence, the stationary regime for the maximum fitness and the sum of fitness within each class is highly contingent on N_A , N_B and their ratio N_A/N_B . Indeed, as N_A/N_B decrease with fixed N_T , the gap is amplified for the minority class, resulting in reduced inequalities within that particular class. However, the gap diminishes for the majority class, giving rise to greater disparities. Our model exhibits a high level of sensitivity to the interactions between agents from opposing classes. If the ratio between the number of agents in both classes shifts, it affects not only the number of interactions but also the fitness values associated with those exchanges.

Figure 7 modifies η . We set a smaller value compared to previous simulations, so that, there is no clear leader in the long run. This result indicates that the model behaves differently depending on the η parameter: we obtain an egalitarian or a hierarchical society depending on η . Figure 8 takes a closer look to this phenomena by considering again the four key indicators in our model: the maximum fitness values of each class, $F_{\max}^A(t)$ and $F_{\max}^B(t)$, and the total fitness for each of one $F_{\text{tot}}^A(t)$ and $F_{\text{tot}}^B(t)$. Results show that η significantly influences the evolution of the indicators. If η is higher, inequalities are magnified, ultimately culminating in the emergence of a single leader within each class of the society.

The exchange factor of fitness, denoted as x , does not impact on the outcomes described. As shown in *Appendix D*, the fitness is however much more stochastic and the time that the system spends to reach a unique leader under certain conditions also varies. If the proportion exchanged is large enough, an agent with small portion of fitness could grow and can lead to a drastic decrease of the fitness of the leader of the opposite class, and so on cyclically. Altering the number of agents in each class and η parameter, while keeping the system size constant, leads to distinct outcomes. These outcomes are further elaborated in the subsequent sections.

To conclude this section, it can be stated that the emergence of a leader or a limited number of leaders in the model is primarily contingent on the values of η and the number of agents (N_A and N_B) and, in turn, the total number of agents N_T , but also on the ratio N_A/N_B . The model describes a shift from an egalitarian to a hierarchical society with changes on η , N_A , N_B and N_A/N_B . On the contrary, the shift does not seem to be caused by changes on the system size L and on the exchange factor x . Table 1 summarizes how the response of the system changes with respect to the mentioned model parameters.

3.2. Quantifying inequalities: the Gini coefficient

The Gini coefficient measures the degree of inequality in a given distribution and indicates how a particular distribution deviates from the uniform distribution. It is usually defined based on the *Lorenz curve*, which shows the proportion of the total income of the population (represented in the vertical axis) that is cumulatively captured by the bottom $x\%$ of the population. The line at 45 degrees represents the perfect equality of a distribution. The Gini

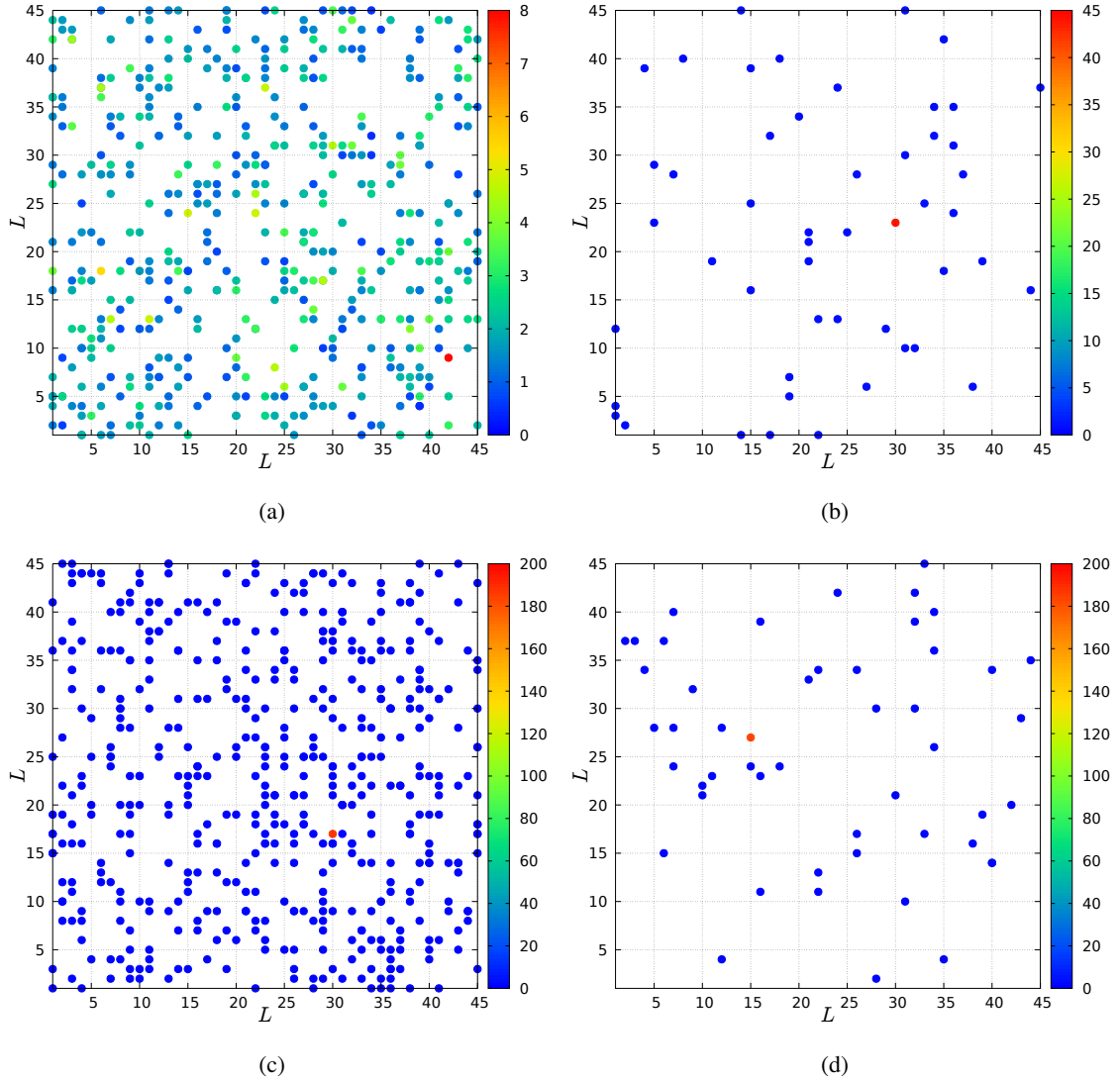


Figure 5: Fitness distribution mapping for the two classes at two distinct times. Fitness heat map of both classes of a single simulation for $N_A = 500$ agents, $N_B = 50$ agents, $\eta = 5$, $x = 0.01$ in a $L \times L$ square lattice with $L = 45$. (a) 20 000 Gillespie time units and class A. (b) 20 000 Gillespie time units and class B. (c) Stationary regime at 600 000 Gillespie time units and class A. (d) Stationary regime at 600 000 Gillespie time units and class B. There can be more than one agent in each site.

coefficient G can be computed as [37]:

$$G = \frac{\sum_{i=1}^n \sum_{j=1}^n |x_i - x_j|}{2 \sum_{i=1}^n \sum_{j=1}^n x_j} = \frac{\sum_{i=1}^n \sum_{j=1}^n |x_i - x_j|}{2n^2 \bar{x}}, \quad (6)$$

where in our model n is the number of individuals in the society, x_i and x_j are the fitness of the individuals i and j , and \bar{x} is the average of the distribution.

Therefore, the Gini coefficient and the Lorenz curve for our simulations can serve to take a closer look at the inequalities as a function of the population for each class (N_A and N_B). Figure 9 shows a fixed system size with the same combinations of N_T and N_A/N_B than in Figure 6.

Emergence of social hierarchies in a society with two competitive classes

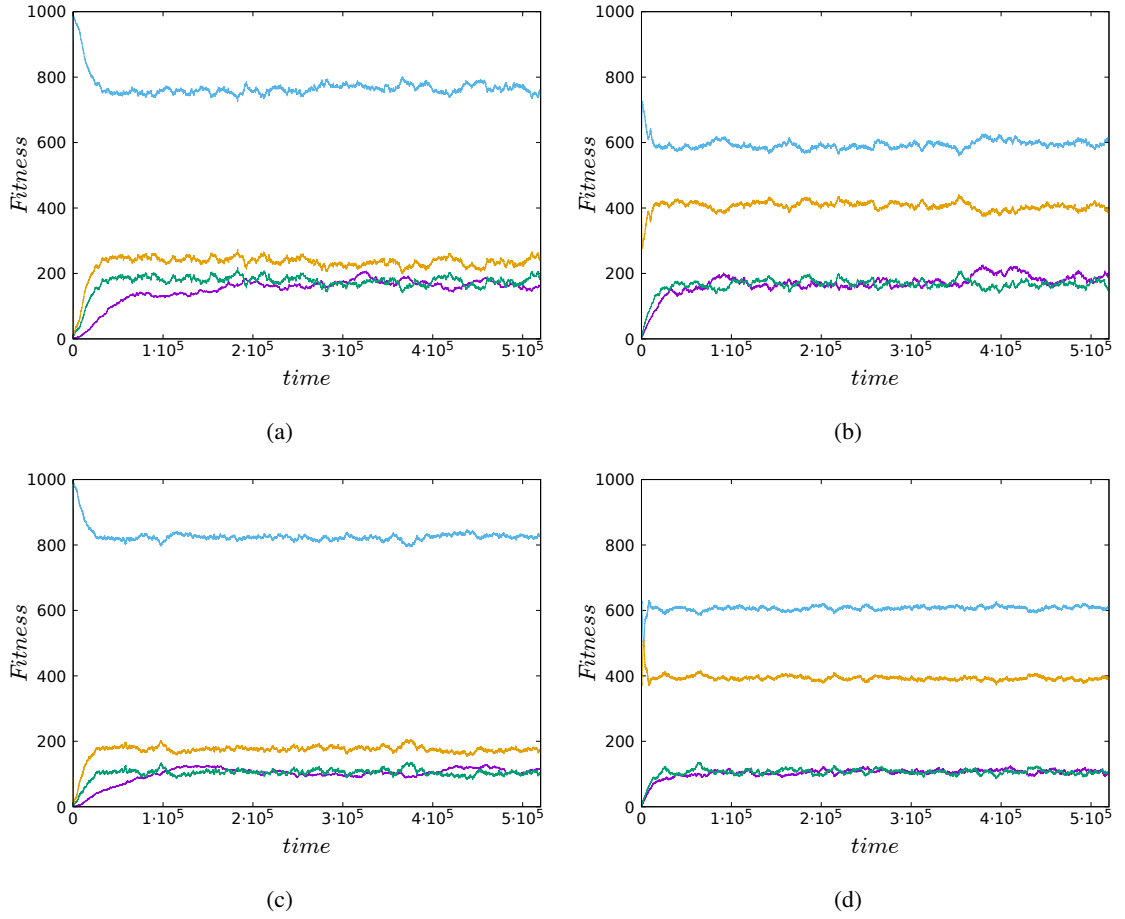


Figure 6: Temporal evolution of key indicators depending on the number of agents. Time evolution of $F_{\max}^A(t)$ (purple), $F_{\max}^B(t)$ (green), $F_{\text{tot}}^A(t)$ (blue) and $F_{\text{tot}}^B(t)$ (yellow) for $\eta = 5$ and $x = 0.01$, randomly simulated on a $L \times L$ lattice ($L = 25$). (a) $N_A = 500$ and $N_B = 50$. (b) $N_A = 350$ and $N_B = 200$. (c) $N_A = 1000$ and $N_B = 100$. (d) $N_A = 700$ and $N_B = 400$.

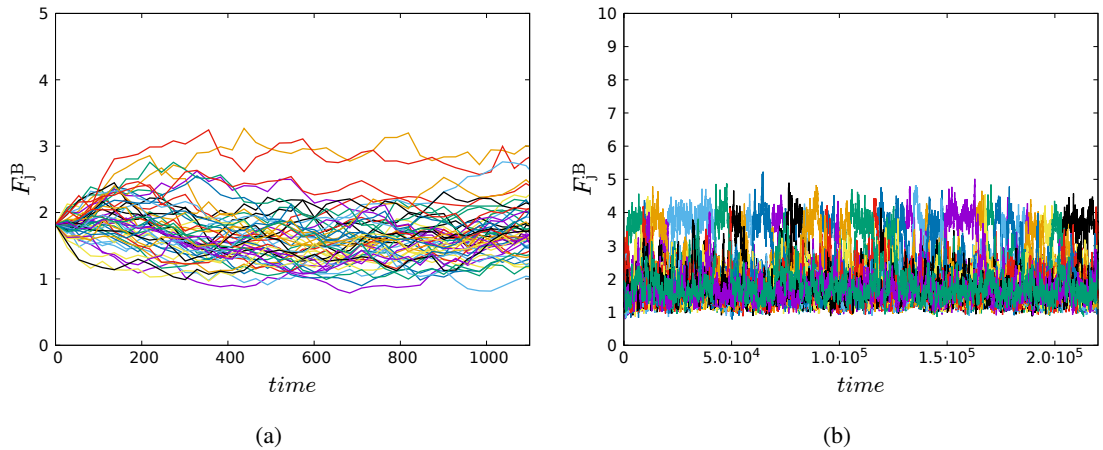


Figure 7: Fitness temporal evolution of one class for smaller η . Time evolution of all F_j^B for $N_A = 500$ and $N_B = 50$ agents, $\eta = 1$ and $x = 0.01$, randomly simulated on a $L \times L$ lattice ($L = 25$). (a) During the first 1100 time steps. (b) Stationary regime.

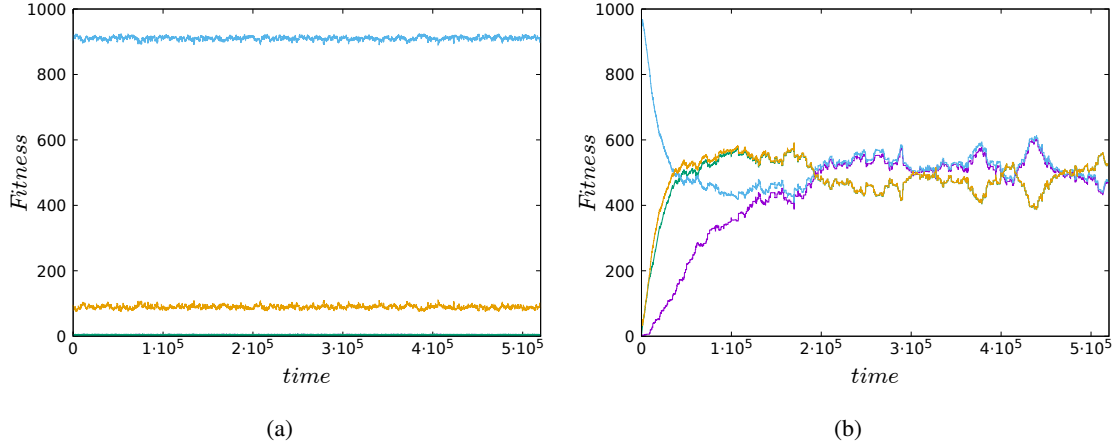


Figure 8: Temporal evolution of key indicators with two different η values. Time evolution of $F_{\max}^A(t)$ (purple), $F_{\max}^B(t)$ (green), $F_{\text{tot}}^A(t)$ (blue) and $F_{\text{tot}}^B(t)$ (yellow) for $N_A = 500$ and $N_B = 50$ agents and $x = 0.01$, randomly simulated on a $L \times L$ lattice ($L = 25$). (a) $\eta = 1$. (b) $\eta = 10$.

Table 1

Dependence on model parameters. The effect of each model parameter on the stationary fitness values and on the time required to reach the stationary regime (“✓” means “it depends” and “–” means “it does not depend”).

Model parameters	Definition	Stationary fitness	Time to stationarity
L	System size	–	✓
η	Interaction intensity	✓	✓
x	Exchange factor	–	✓
N_A & N_B	Number of agents in class A and B	✓	✓
N_T	Total number of agents in the society	✓	✓
ϕ	Overall fitness of the entire society	–	–
$F_i^A(0)$ & $F_i^B(0)$	Initial fitness values	–	✓
ω_i^A & ω_j^B	Gillespie movement rates for agents in class A and B (Defined in the Appendices)	–	✓

It is evident that inequalities are highly sensitive to the number of agents that conform each class. Specifically, inequalities consistently appear more pronounced within the smaller group. Upon examining both classes depicted in Figure 9 (a) and Figure 9 (c), we observe that doubling N_T while maintaining $N_A/N_B = 10$ constant, leads to decreased inequalities within the minority group, the majority group and the overall society. Conversely, when holding the total society size $N_T = 550$ constant, while the fraction $N_A/N_B = 1.75$ is lowered, Figure 9 (b) shows that we can notably reduce inequalities within the minority class by slightly augmenting inequalities within the majority class. Interestingly, the inequalities within the entire system remain relatively unchanged in this scenario. A notable observation is that in all subfigures, there is a final large step attributable to the presence of a leader in each class. The height of this step provides information about the value of the maximum fitness. Particularly, the size represents the percentage of F_{\max}^A within its class, and the same for class B.

The Gini coefficient study reveals that inequality levels are significantly influenced by the population size of each class within a society. Precisely, inequalities are more pronounced in smaller groups. When the total population size is doubled while maintaining a fixed class ratio, inequalities decrease in both the minority and majority groups, as well as in the overall society. However, when the total population remains constant, but the class ratio is decreased making the classes more similar in size, inequalities within the minority group can be substantially reduced, even if this slightly increases inequalities within the majority group, without significantly affecting the overall societal inequality. This indicates that managing class sizes and ratios is a key factor in addressing and mitigating inequalities within a population.

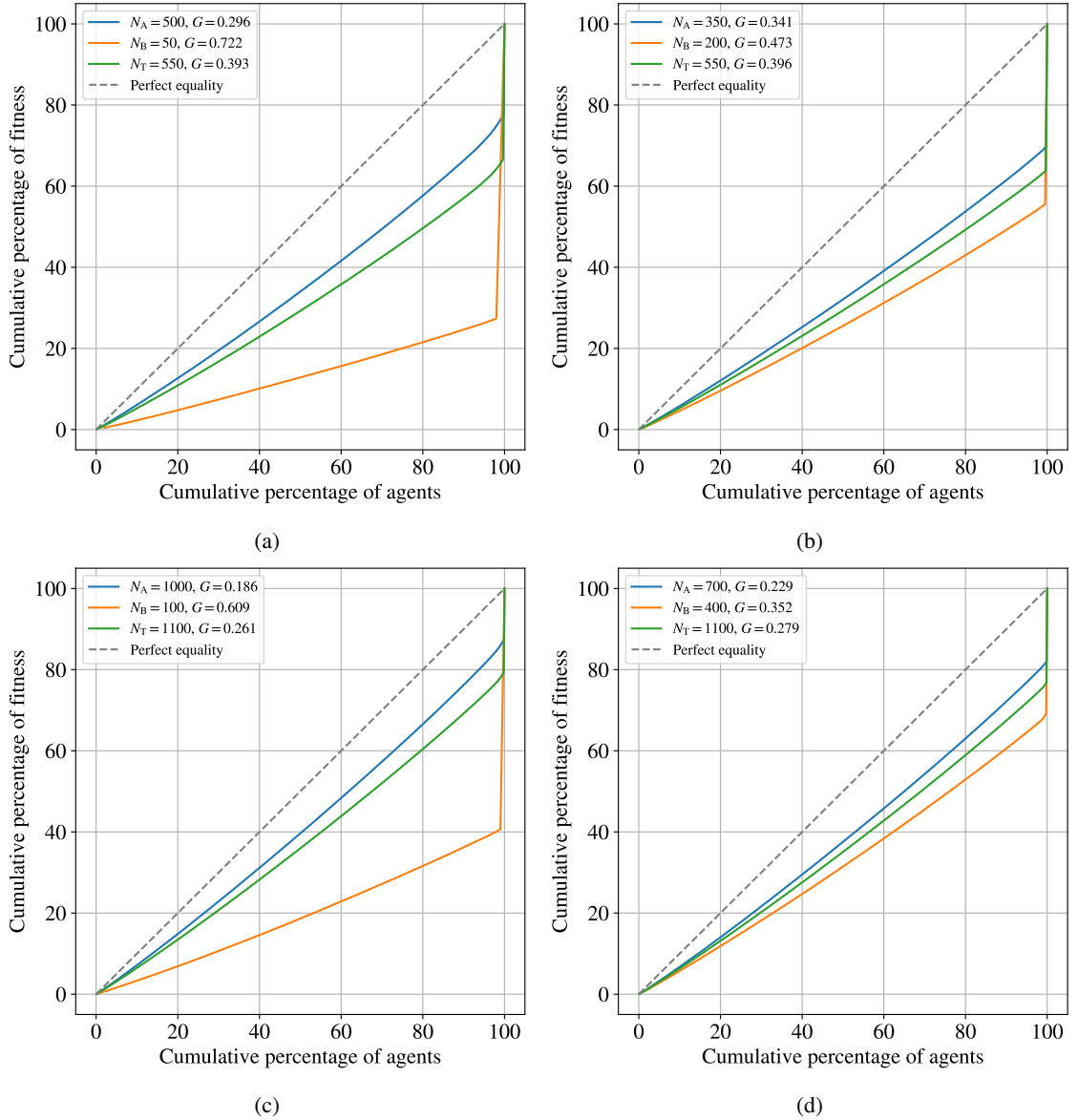


Figure 9: Lorenz curves and Gini coefficients for different number of agents. Lorenz curves and Gini coefficients of one single trajectory at the stationary regime for $\eta = 5$ and $x = 0.01$, randomly simulated on a $L \times L$ lattice ($L = 25$). (a) $N_A = 500$ and $N_B = 50$. (b) $N_A = 350$ and $N_B = 200$. (c) $N_A = 1000$ and $N_B = 100$. (d) $N_A = 700$ and $N_B = 400$.

4. The role of η

We now study F_{\max}^A , $F_{\max}^A / F_{\text{tot}}^A$ and F_{tot}^A for the stationary regime and as a function of η . We repeat the analysis for several combinations of the number of agents N_A and N_B , and also for the other class B. The results are sampled 250 times during the stationary regime within a single simulation, each taken every 1000 Gillespie time units. Data presented is also subject to an additional average across 50 simulations. To ensure normalized results, we set ϕ to 1 arbitrary unit for all simulations presented until the end.

Figure 10 (a) shows the maximum agent fitness of each class as a function of η . Essentially, these fitnesses represent the values of the leaders of each class. Figure 10 (a) shows a possible phase transition; from an egalitarian society ($\eta = 0$ all the agents have the same probability to win independent of their fitness, cf. Equation (3)) to a hierarchical society, large η , one leader in each class is acquiring almost all the fitness, converging towards the common value

of $1/2$, regardless of the number of agents N_A and N_B . For different combinations of N_A and N_B , F_{\max}^A and F_{\max}^B evolve consistently with respect to η . This observation underscores that the leadership appearance remains unaffected by changes in the number of agents within each class. Nevertheless, curves shift towards large η when the total number N_T increases. Indeed, for societies composed by the same N_T , all curves overlap. This provides an initial insight into how these trends are influenced by η and N_T . Finally, for sufficient large values of η , all considered examples of the observable collapse. We wonder if this is still true in the thermodynamic limit, that is, for $N_T \rightarrow \infty$, thus defining a critical value for η . Due to computational constraints, this study was unable to address this question.

Figure 10 (b) represents the maximum agent fitness within each class, normalized by the total fitness of all agents within the same class. In essence, it signifies the leadership status within each class. Similar to the observation in Figure 10 (a), a shift from an egalitarian to a hierarchical societal behaviour becomes apparent. Near $\eta = 0$, this corresponds to the scenario with maximal equality, where all agents within their respective class possess the same fitness $1/N_A$, and likewise for the other class. On the opposite side, for large η , a clear leader emerges in each population. In this scenario, the curves shift towards the right as the number of agents N_A (or N_B) increases. The curves are superimposed if the value of the number of agents is the same, regardless if corresponds to N_A (the larger group) or N_B (the smaller one). Once again, the question is whether the curves continue their rightward movement indefinitely or reach a point where they cease to shift at a certain N_A and N_B .

Finally, Figure 10 (c) shows the total fitness of each class as a function of the parameter η . The evolution of this observable exhibits some peculiarities. At small values of η , all individuals possess identical fitness, and consequently, this point is directly proportional to the number of agents in each class. Essentially, it is given by N_A/N_T , and the same for the other class. Hence, if the ratio N_A/N_B is equal, simulations converge to the same value at $\eta = 0$. In contrast to previous observations, the behaviour of the curves is diverse depending on the number of agents. Also, looking at larger η , it seems to exist a singular η around 8 that increases with N_T , where the fitness distribution between classes does not depend on the number of individuals. In this case, each class shares an equal amount of fitness.

All in all, results provided in Figure 10 suggests that from a particular η value onwards, a significant portion of the total fitness is primarily kept by the leader individuals. As we mention above, we do not have enough computational power to find the thermodynamic limit. The question that arises at this point is what analytical functional dependence have all these observables in relation to η and the number of agents.

5. Scaling laws

We first investigate how the maximum agent fitness and the maximum agent fitness normalized by the total fitness of all agents within the same class, can be represented by the same curve, regardless of the number of agents. Both quantities have the same sigmoidal shape as a function of η . We thus suggest a sigmoidal fit of F_{\max}^A for several values of N_T (see Figure 10 (a)):

$$g(\eta, N_T) = \frac{1}{2 + e^{-a_0^g(N_T)(\eta - \eta_0^g(N_T))}}. \quad (7)$$

We also suggest another (very similar) sigmoid fit of $F_{\max}^A/F_{\text{tot}}^A$ for several values of N_A (see Figure 10 (b)):

$$h(\eta, N_A) = \frac{1}{1 + e^{-a_0^h(N_A)(\eta - \eta_0^h(N_A))}}. \quad (8)$$

The same expressions would apply for the class B. We can then estimate a_0^g and η_0^g as a function of N_T , and a_0^h and η_0^h as a function of N_i , to see their dependence on the number of agents. The fitted parameters behave as follows:

$$\begin{aligned} a_0^g &\approx 1 \quad \forall N_T \\ \eta_0^g(N_T) &= \ln(N_T - 2) \\ a_0^h &\approx 1 \quad \forall N_A \\ \eta_0^h(N_A) &= \ln(N_A - 1). \end{aligned} \quad (9)$$

And the same relationships for the class B. The reason for these -2 and -1 values inside the logarithms are in order to satisfy the boundary condition for $\eta = 0$, where the fitted functions have to take the values of $1/N_T$ and $1/N_A$ (or $1/N_B$), the so-called the egalitarian society.

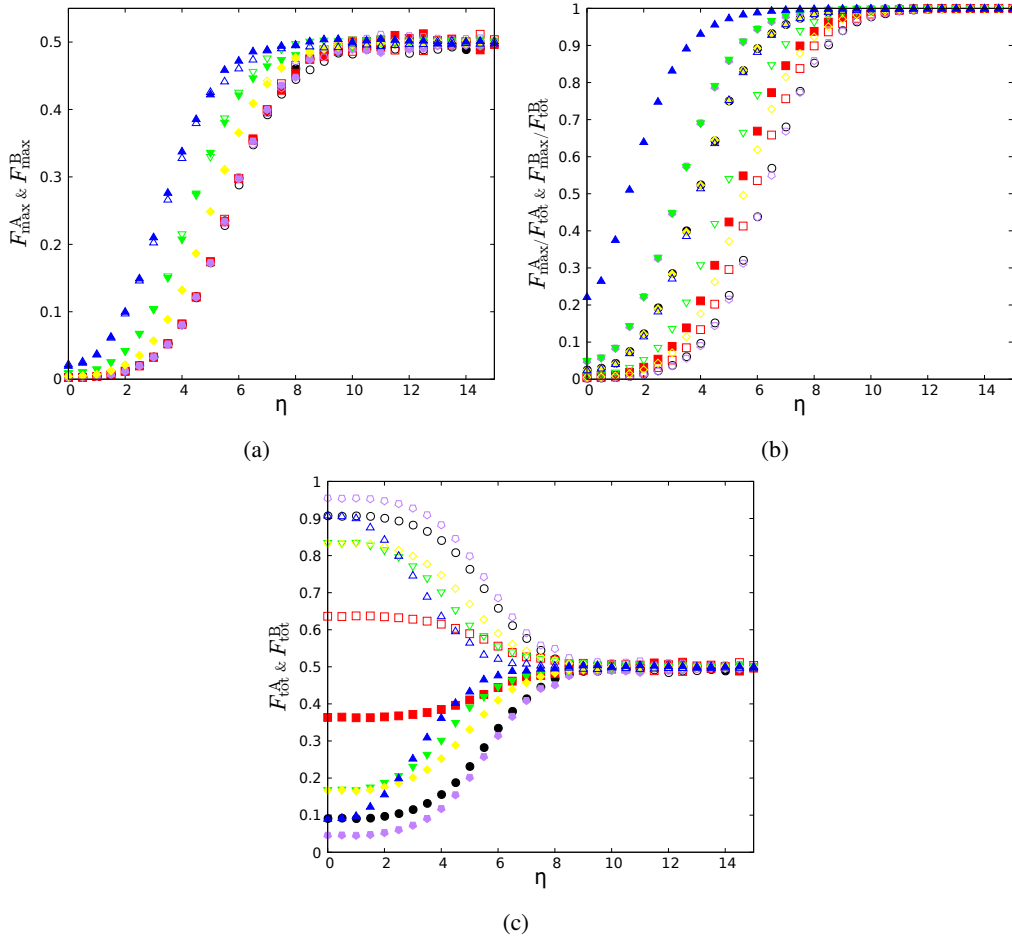


Figure 10: Total fitness and maximum fitness as a function of η . The class A (empty symbols) and the class B (filled symbols) are in all cases plotted as a function of the parameter η , for $L = 25$ and $x = 0.01$: (a) Maximum agent fitness of each class. (b) Maximum agent fitness of each class normalized by the sum of all agent fitness of the same class. (c) Total fitness of each class. The simulations have been done for $N_A = 500$ and $N_B = 50$ (black circles), $N_A = 350$ and $N_B = 200$ (red squares), $N_A = 525$ and $N_B = 25$ (purple pentagons), $N_A = 125$ and $N_B = 25$ (green down triangles), $N_A = 250$ and $N_B = 50$ (yellow rhombuses), $N_A = 50$ and $N_B = 5$ (blue up triangles). Error bars are depreciable.

Functions F_{\max}^A and $F_{\max}^A/F_{\text{tot}}^A$ can be therefore effectively described by sigmoidal functions depending on the free parameter η , the total number of agents N_T , and the number of agents in each class as:

$$F_{\max}^A(\eta, N_T) = \frac{1}{2 + (N_T - 2)e^{-\eta}}, \quad (10)$$

$$\frac{F_{\max}^A}{F_{\text{tot}}^A}(\eta, N_A) = \frac{1}{1 + (N_A - 1)e^{-\eta}}, \quad (11)$$

and the same expressions apply for the class B. These sigmoidal shapes can be related to a phase transition from egalitarian to hierarchical societies for each class as a function of the control parameter η . Figure 11 shows a phase diagram of the Equation (11) to see this clear behavioural change depending on these both parameters. In the blue region, the absence of a leader is observed, whereas transitioning to the yellow region signifies the emergence of either multiple leaders or a predominant leader, ultimately culminating in the establishment of a singular leader within the yellow region.

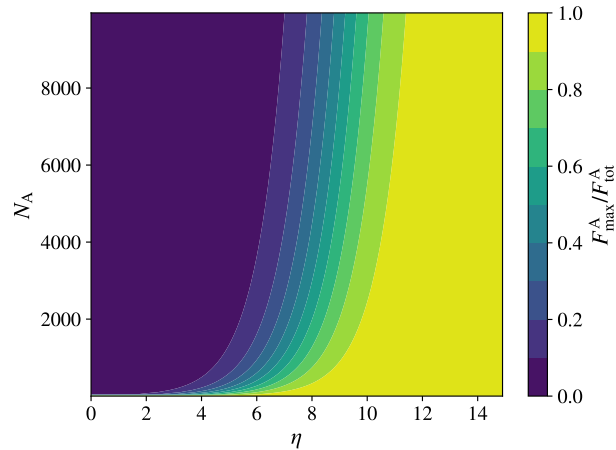


Figure 11: Heat map of the scaling function for the maximum fitness normalized by the sum agent fitness. 2D plot of the scaling function given by Equation (11) in colour, as a function of the parameters η and the number of agents of the class A.

Unfortunately, the curve depicted in Figure 10 (c) lacks a clear functional representation based on the number of individuals in each class. Finding a mathematical equation to explain this behaviour can become an interesting investigation in a future work.

6. Concluding remarks

The formation of hierarchies in societies is an intriguing topic in which agent-based modelling approach can provide important insights. Hierarchies are assumed to be built in a bottom-up approach and based on interactions between agents. Hierarchies are widely present in human societies, and they appear in contexts such as cities where interactions intensively take place [19]. The formation of hierarchies in urban areas has serious consequences in terms of segregation and inequality [20, 38]. Cities are organized in systematic manners [39, 40] and they shape human interactions [41, 42]. In fact, face-to-face interaction is a basic human behaviour, modelling how people form and keep social groups by segregating themselves from others [43–46]. The lack of social cohesion can undermine the social fabric of cities and dramatically affect the economic, social and health conditions of people living in urban areas [47, 48]. Macroscopic social hierarchies can spontaneously emerge from micro-motives in human daily habits. Measurable attributes such as income, education, occupation, and wealth are used as indicators of socioeconomic status, either individually or in combination to create composite indicators of socioeconomic standing [49]. However, our knowledge of the interplay between group dynamics and the emergence of inequalities in social systems is still limited and quantitatively researched [50]. Although there are many studies on the tendency of human beings to form groups that are socially cohesive, the lack of large-scale data has left many questions about social groups undetermined. For instance, in [21] the study of the nature of urban groups and a methodology for their identification is developed thanks to anonymized mobile phone datasets, such as Call Detail Records.

A better understanding of the formation of hierarchies and their consequences is what has motivated us to extend the Bonabeau model by introducing a second class in the society. The model only allows for interactions among agents that belong to different classes. Under certain conditions, Monte Carlo simulations show that for a broad range of values of the model, the fitness of the agents of each class present a decay in time except for one or few agents which capture almost all the fitness of the system. A clear behavioural change in several ways of representing the fitness of the system is observed when the control parameter η is changed. The phenomena can be understood as a phase transition from an egalitarian to a hierarchical society. The results remain robust with respect to the system size and depend solely on the number of agents within each class and their ratio. In contrast to the original Bonabeau model [22], our model shows that the degree of the inequalities do not depend on the overall density of individuals in the society or within each class. Instead, it is determined by the number of individuals and it is then basically a question of number of interactions. Scaling functions for the maximum agent fitness, as well as for the maximum agent fitness normalized by

the sum of all agent fitness within the same class, are found and the mathematical expressions obtained can be useful to extend the results to larger systems.

The model may be related to different real-world situations and it is thus possible to further reflect on the outcomes under certain circumstances. The lattice might be a proxy of a city in which inhabitants are constantly moving around. One can imagine that the two classes represent people and businesses and the only interactions possible are transactions among people and businesses. Then we can look at different scenarios for businesses. For small η , all businesses share the same fitness, which this situation is known as *perfect competition*. Increasing η , a dominant business emerges, but not with all the fitness of its class. We are in the *monopolistic competition* regime and an *oligopoly* gives rise. Finally, when η is large enough, all fitness is concentrated into to a single business (a *monopoly*). The same reasoning might apply with two competing criminal gangs sharing the same physical space (eventually a city). The model might thus be telling us that the more fights the more important would be the role of each gang leader while other members of each gang would be those losing all fitness and all power or wealth. Another situation which is becoming more and more frequent is the competition for urban space between tourists and neighbors and just by the existence of these interactions many side-effects are just happening such as gentrification of the center of the cities. In this case, the model can help to further reflect how only few of each of class (tourists and neighbours) hold most of the privileges. Other situations can be also imagined when two very different social groups are in interaction. To compare numerical simulations of the model with real data is expected to be a future work, by for instance taking household income as a proxy for societal status in a city [33, 51].

The model can be extended in many ways such as other winners' probabilities [33, 52], the redistribution of the total fitness applying a relaxation term in the temporal evolution rules, and so on. It is indeed possible to add other sort of interactions, to allow other movements (not only a random walk) or to add constraints [27–29, 53], to use time-varying networks [54] and even to increment the number of classes. Also, game-theoretical models capture very flexible situations where cooperation among selfish agents can emerge [55, 56] and analytical studies could be implemented [25].

CRediT authorship contribution statement

Marc Sadurní: Conceptualization, Methodology, Writing. Original draft. **Josep Perelló:** Supervision, Writing. Review & editing. **Miquel Montero:** Supervision, Writing. Review & editing.

Competing interests

The authors declare no competing interests.

Acknowledgments

This work has been partially funded by MCIN/AEI/ 10.13039/501100011033, grant number PID2019-106811GB-C33 (JP and MM); by MCIN/AEI/ 10.13039/501100011033 and by “ESF Investing in your future”, grant number PRE2020-093266 (MS); by MCIN/AEI/ 10.13039/501100011033 and by “ERDF A way of making Europe”, grant number PID2022-140757NB-I00. We also acknowledge the support of Generalitat de Catalunya, grant number 2021SGR00856.

Appendices

A. Fitness normalization

To compare the prestige/reputation between two agents of opposite classes when a random interaction happens, we normalize them under their respectively sample. Therefore, when an exchange is possible, performing this normalization we will not compare directly the fitness but their prestige which each has into its particular class. We have proved the following scenarios:

1. Scaling (min-max normalization):

$$\hat{F}_j^B(t) = \frac{F_j^B(t) - F_{\min}^B(t)}{F_{\max}^B(t) - F_{\min}^B(t)}, [0, 1] \quad (12)$$

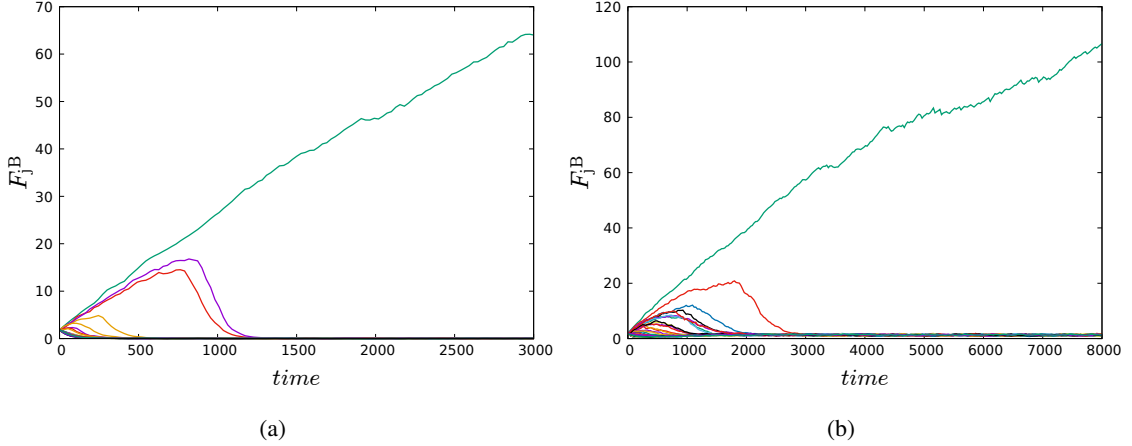


Figure 12: Temporal evolution of the fitnesses of class B for two different normalizations. Time evolution of all F_j^B for $N_A = 500$ and $N_B = 50$ individuals, $\eta = 5$ and $x = 0.01$, randomly simulated on a $L \times L$ lattice ($L = 25$) and two different normalizations. (a) The first 3 000 time steps using the linear scaling to a range of $[-1, 1]$. (b) The first 8 000 time steps using the mean normalization.

2. Linear scaling to a range:

$$\hat{F}_j^B(t) = a + \frac{(F_j^B(t) - F_{\min}^B(t))(b - a)}{F_{\max}^B(t) - F_{\min}^B(t)}, [a, b] \quad (13)$$

3. Mean normalization:

$$\hat{F}_j^B(t) = \frac{F_j^B(t) - \langle F_j^B(t) \rangle}{F_{\max}^B(t) - F_{\min}^B(t)} \quad (14)$$

where a and b are free integer numbers and $\langle F_j^B(t) \rangle$ is the mean of the fitnesses vector. And the same equations for $\hat{F}_i^A(t)$. In Figure 3 (a) and Figure 12, we show that applying these three types of normalizations, the results are qualitatively the same. For simplicity, we have chosen the first one, Equation (12).

B. Monte Carlo methods

In this Appendix, a brief review of the Monte Carlo setup is explained:

1. The lattice is equipped by Periodic Boundary Conditions (PBC). In terms of a city, this could be understood as a simplification of that people travelling from in to out of the city, and vice versa.
2. A residence time algorithm, also called Gillespie algorithm, is applied to reproduce the time when a jump happens [35]. The movement rate of each agent of the class A, ω_i^A , is settled to 1, and the same for the class B, $\omega_j^B = 1$. Therefore, the total rate when a given agent of the first class moves is $\Omega_A = N_A \omega_i^A = N_A$ and the same for the second class $\Omega_B = N_B \omega_j^B = N_B$. Then, the global rate Ω_T when any move happens corresponds to the sum of both: $\Omega_T = \Omega_A + \Omega_B$. The time t in our simulations will be in units of ω , and the time step to the next movement is randomly simulated as:

$$\Delta t = -\frac{\ln u}{\Omega_T}, \quad (15)$$

where $u \sim U(0, 1)$ is a uniform random number between 0 and 1. After given that a movement has occurred, we randomly identify which class of agent performs it according to the total rates of class A and B. If the movement rates of all agents of one class would settle to zero, the system could be understood as a business-client interaction, where one of the two classes is static.

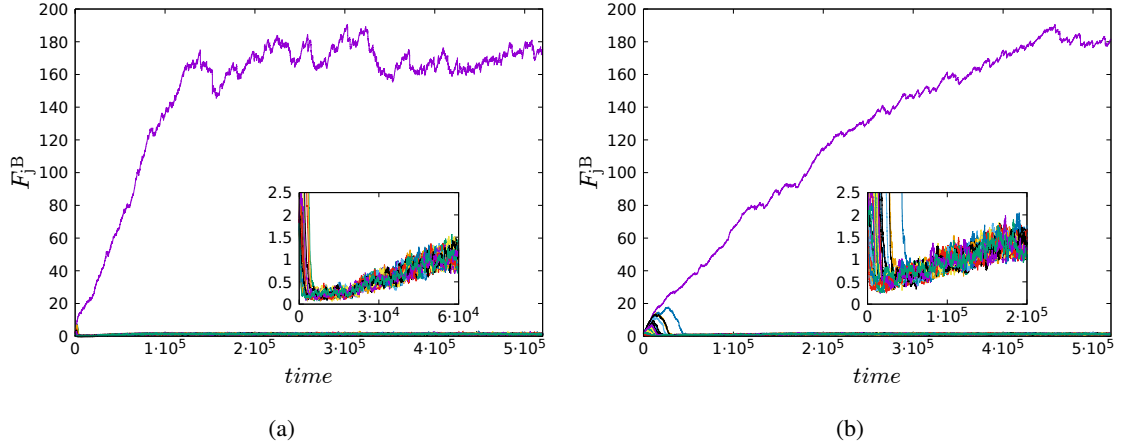


Figure 13: Temporal evolution of the fitnesses of class B for two systems sizes, $\eta = 5$ and $x = 0.01$. Time evolution of all F_j^B for $N_A = 500$ and $N_B = 50$ individuals, $\eta = 5$ and $x = 0.01$, randomly simulated on two 2D lattice sizes. (a) $L = 65$, (b) $L = 120$.

3. We register one point every $N_{\text{movements}}$ or dt to reduce storage needs.
4. We have observed that changing the initial distribution of fitness among the agents, the tendency towards the stationary regime does not change.

C. System size dependence

We here illustrate the connection between the stationary regime and the system size, as well as its dependence on the time required to reach this state. First, trajectories for the fitness of the class B are plotted for two distinct values of the system size L in Figure 13. We see how the leader appears lately (the second case) as well as the time required to reach the stationary regime.

Besides, in Figure 14 we compute the stationary numerical times for many system sizes. We have obtained these times by averaging over 100 different runs when the maximum value in the class reaches the average maximum fitness computed in this stationary regime. For the parameters showed in Figure 14, the average value of the maximum fitness of the class B computed in the stationary regime for all L is around 175 (see Figure 4). The obtained values for these particular parameters of the model from the least squares fit $t \sim aL^b$ have been: $a = 39.5 \pm 4.0$ and $b = 2.0 \pm 0.1$. Therefore, this scaling behaviour could be interpreted as a diffusion process of the agents' fitness in the space, where larger is the territory larger is the time to have an encounter, and consequently, larger the time of leader emergence.

D. Exchange factor dependence

Below, we present the relationship between the temporal evolution of fitness and the exchange factor denoted as x . Figure 15 illustrates the temporal evolution of fitnesses of class B during the stationary regime for two distinct values of x , while maintaining the same parameters as Figure 3. As discussed in the main text, a comparison between Figure 3 (b) and Figure 15 (a) reveals that the time taken to reach the stationary regime significantly decreases with increasing x , albeit with a notable increase in stochasticity within this regime. With further increments in x , as depicted in Figure 15 (b), the exchange factor becomes sufficiently large to result in the emergence of agents with lower fitness levels upon encounters with more powerful agents of the opposing class A, and vice versa.

References

- [1] M. Steinbacher, M. Raddant, F. Karimi, E. Camacho Cuenca, S. Alfarano, G. Iori, T. Lux, Advances in the agent-based modeling of economic and social behavior, SN Business & Economics 1 (2021) 99.
- [2] B. J. Alder, T. E. Wainwright, Phase transition for a hard sphere system, The Journal of Chemical Physics 27 (1957) 1208.
- [3] B. J. Alder, T. E. Wainwright, Studies in molecular dynamics. i. general method, The Journal of Chemical Physics 31 (1959) 459.

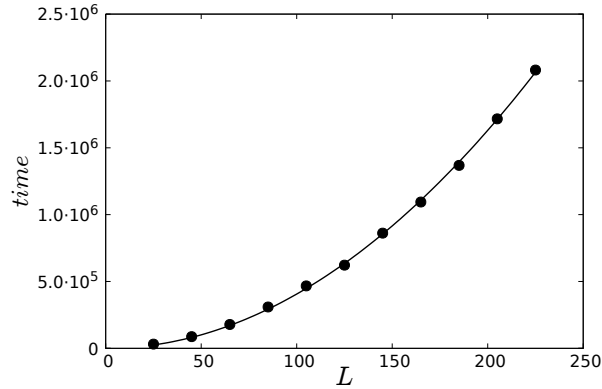


Figure 14: Scaling time when a dominant agent of the class B reach the stationary regime as a function of the system size. Scaling time when the maximum fitness value of the class B reaches the average stationary value as a function of the system size L , for $N_A = 500$ and $N_B = 50$ individuals, $\eta = 5$ and $x = 0.01$. Numerical values averaged under 100 different runs (filled circles) and a potential fit of the form: $t \sim aL^b$ (solid line) is plotted. Error bars are depreciable.

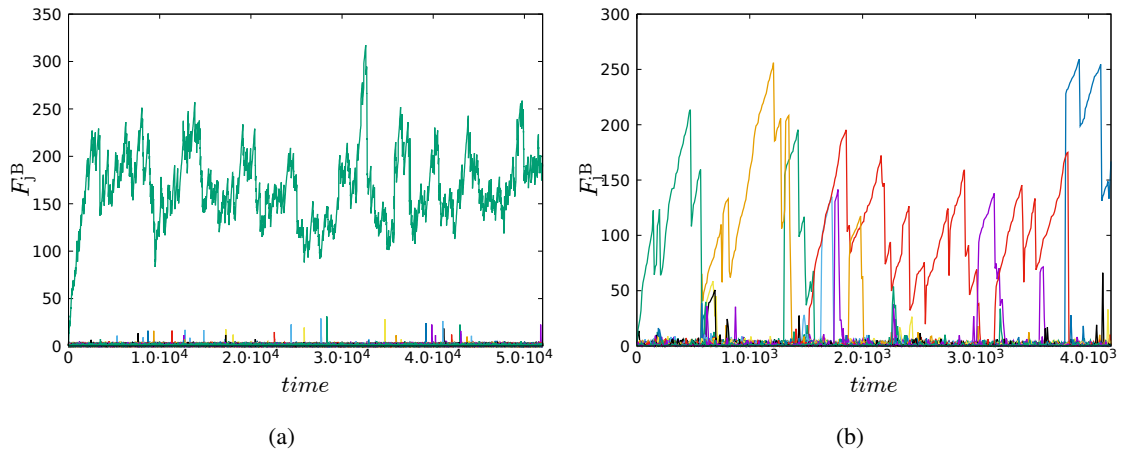


Figure 15: Temporal evolution of the fitnesses of class B with two values of x . Time evolution of all F_j^B for $N_A = 500$ and $N_B = 50$ individuals, $\eta = 5$, randomly simulated on a $L \times L$ lattice ($L = 25$) and two different exchange factors. (a) $x = 0.10$. (b) $x = 0.50$.

[4] N. Metropolis, A. Rosenbluth, M. Rosenbluth, A. Teller, E. Teller, Equation of state calculations by fast computing machines, *The Journal of Chemical Physics* 21 (1953) 1087.

[5] M. Jusup, P. Holme, K. Kanazawa, M. Takayasu, I. Romić, Z. Wang, S. Geček, T. Lipić, B. Podobnik, L. Wang, W. Luo, T. Klanjšček, J. Fan, S. Boccaletti, M. Perc, *Social physics, Physics Reports* 948 (2022) 1–148.

[6] D. Lazer, A. Pentland, L. Adamic, S. Aral, A. L. Barabási, D. Brewer, N. Christakis, N. Contractor, J. Fowler, M. Gutmann, T. Jebara, G. King, M. Macy, D. Roy, M. Van Alstyne, *Computational social science, Science* 323 (2009) 721–723.

[7] C. Castellano, S. Fortunato, V. Loreto, *Statistical physics of social dynamics, Reviews of Modern Physics* 81 (2009) 591–646.

[8] W. C. Allee, Social dominance and subordination among vertebrates. levels of integration in biological and social systems, *Biology Symposium* 8 (1940) 139.

[9] H. G. Landau, On dominance relations and the structure of animal societies: I. effect of inherent characteristics, *The bulletin of mathematical biophysics* 13 (1951) 1–19.

[10] A. Guhl, Social inertia and social stability in chickens, *Animal Behaviour* 16 (1968) 219–232.

[11] I. D. Chase, Social process and hierarchy formation in small groups: A comparative perspective, *American Sociological Review* 45 (1980) 905–924.

[12] E. O. Wilson, *The insect societies*, Harvard University Press, Cambridge, MA, 1971.

- [13] C. Goessmann, C. Hemelrijk, R. Huber, The formation and maintenance of crayfish hierarchies: behavioral and self-structuring properties, *Behavioral Ecology and Sociobiology* 48 (2000) 418–428.
- [14] I. D. Chase, C. Tovey, D. Spangler-Martin, M. Manfredonia, Individual differences versus social dynamics in the formation of animal dominance hierarchies, *Proceedings of the National Academy of Sciences* 99 (2002) 5744.
- [15] W. B. Lindquist, I. D. Chase, Data-based analysis of winner-loser models of hierarchy formation in animals, *Bulletin of mathematical biology* 71 (2009) 556.
- [16] R. M. Wittig, C. Boesch, Food competition and linear dominance hierarchy among female chimpanzees of the tai national park, *International Journal of Primatology* 24 (2003) 847.
- [17] R. C. Savin-Williams, Dominance hierarchies in groups of middle to late adolescent males, *Journal of Youth and Adolescence* 9 (1980) 75.
- [18] C. Garandeau, I. Lee, C. Salmivalli, Inequality matters: classroom status hierarchy and adolescents' bullying., *Journal of Youth and Adolescence* 43 (2014) 1123.
- [19] E. Moro, D. Calacci, X. Dong, A. Pentland, Mobility patterns are associated with experienced income segregation in large us cities, *Nature Communications* 12 (2021) 4633.
- [20] J. Checa, O. Nel-lo, Residential segregation and living conditions. an analysis of social inequalities in catalonia from four spatial perspectives, *Urban Science* 5 (2021) 45.
- [21] M. Zignani, C. Quadri, S. Gaito, G. P. Rossi, Urban groups: behavior and dynamics of social groups in urban space, *EPJ Data Science* 8 (2019) 8.
- [22] E. Bonabeau, G. Theraulaz, J. Deneubourg, Phase diagram of a model of self-organizing hierarchies, *Physica A: Statistical Mechanics and its Applications* 217 (1995) 373–392.
- [23] I. D. Chase, C. Bartolomeo, L. A. Dugatkin, Aggressive interactions and inter-contest interval: how long do winners keep winning?, *Animal Behaviour* 48 (1994) 393.
- [24] D. Stauffer, Phase transition in hierarchy model of bonabeau, *International Journal of Modern Physics C* 14 (2003) 237.
- [25] L. Lacasa, B. Luque, Bonabeau hierarchy models revisited, *Physica A: Statistical Mechanics and its Applications* 366 (2006) 317–322.
- [26] K. Malarz, D. Stauffer, K. Kulakowski, Bonabeau model on a fully connected graph, *The European Physical Journal B - Condensed Matter and Complex Systems* 50 (2006) 195–198.
- [27] T. Odagaki, M. Tsujiguchi, Self-organizing social hierarchies in a timid society, *Physica A: Statistical Mechanics and its Applications* 367 (2006) 435–440.
- [28] M. Tsujiguchi, T. Odagaki, Self-organizing social hierarchy and villages in a challenging society, *Physica A: Statistical Mechanics and its Applications* 375 (2007) 317–322.
- [29] M. Pósfai, R. M. D'Souza, Talent and experience shape competitive social hierarchies, *Physical Review E* 98 (2018) 020302.
- [30] E. Ben-Naim, S. Redner, Dynamics of social diversity, *Journal of Statistical Mechanics: Theory and Experiment* 2005 (2005) L11002–L11002.
- [31] E. Ben-Naim, F. Vazquez, S. Redner, On the structure of competitive societies, *The European Physical Journal B - Condensed Matter and Complex Systems* 49 (2006) 531–538.
- [32] T. Miyaguchi, T. Miki, R. Hamada, Piecewise linear model of self-organized hierarchy formation, *Physical Review E* 102 (2020) 032213.
- [33] J. Hickey, J. Davidsen, Self-organization and time-stability of social hierarchies, *PLOS ONE* 14 (2019) e0211403.
- [34] R. Prieto-Curiel, G. M. Campedelli, A. Hope, Reducing cartel recruitment is the only way to lower violence in mexico, *Science* 381 (2023) 1312–1316.
- [35] R. Toral, P. Colet, *Stochastic numerical methods: An introduction for students and scientists*, John Wiley & Sons (2014).
- [36] M. S. Parera, BonabeauExtendedModel, 2024. URL: <https://github.com/MarcSadurniParera/BonabeauExtendedModel.git>, accessed: 15 May, 2024.
- [37] Y. Amiel, F. Cowell, *Thinking about inequality: Personal judgment and income distributions*, Cambridge University Press, 1999.
- [38] L. Espín-Noboá, C. Wagner, M. Strohmaier, F. Karimi, Inequality and inequity in network-based ranking and recommendation algorithms, *Scientific Reports* 12 (2022) 2012.
- [39] L. M. Bettencourt, The origins of scaling in cities, *Science* 340 (2013) 1438.
- [40] L. M. Bettencourt, *Introduction to urban science: evidence and theory of cities as complex systems*, MIT Press, 2021.
- [41] M. Oliveira, C. Bastos-Filho, R. Menezes, The scaling of crime concentration in cities, *PloS one* 12 (2017) 8.
- [42] J. Lobo, L. M. Bettencourt, M. E. Smith, S. Ortmann, Settlement scaling theory: bridging the study of ancient and contemporary urban systems, *Urban Studies* 57 (2020) 731.
- [43] E. Goffman, *Interaction Ritual: Essays On Face-to-face Interaction*, Aldine, 1967.
- [44] A. Kendon, R. M. Harris, M. R. e. Key, *Organization of Behavior in Face-to-face Interaction*, Mouton Publishers, 1975.
- [45] S. Duncan, D. W. Fiske, *Face-to-face Interaction: Research, Methods, and Theory*, Lawrence Erlbaum Associates, 1977.
- [46] F. Bargiela-Chiappini, M. e. Haugh, *Face, Communication and Social Interaction*, Equinox Publishing Ltd, 2009.
- [47] R. Florida, *The New Urban Crisis: How Our Cities Are Increasing Inequality, Deepening Segregation, and Failing the Middle Class-and What We Can Do About It*, Basic Books, 2017.
- [48] L. Finneran, M. Kelly, Social networks and inequality, *Journal of Urban Economics* 53 (2003) 282–299.
- [49] L. S. Vickie, Measurement of socioeconomic status in health disparities research, *Journal of the National Medical Association* 99(9) (2007) 1013–23.
- [50] M. Oliveira, F. Karimi, M. Zens, J. Schaible, M. Génois, M. Strohmaier, Group mixing drives inequality in face-to-face gatherings, *Communications Physics* 5 (2022) 127.
- [51] B. Hong, B. J. Bonczak, A. Gupta, C. E. Kontokosta, Measuring inequality in community resilience to natural disasters using large-scale mobility data, *Nature Communications* 12 (2021) 1870.
- [52] S. Ispolatov, P. Krapivsky, S. Redner, Wealth distributions in asset exchange models, *The European Physical Journal B - Condensed Matter and Complex Systems* 2 (1998) 267–276.

- [53] A. Woolcock, C. Connaughton, Y. Merali, F. Vazquez, Fitness voter model: Damped oscillations and anomalous consensus, *Physical Review E* 96 (2017) 032313.
- [54] M. Kawakatsu, P. S. Chodrow, N. Eikmeier, D. B. Larremore, Emergence of hierarchy in networked endorsement dynamics, *Proceedings of the National Academy of Sciences* 118 (2021).
- [55] S. Lee, P. Holme, Z.-X. Wu, Cooperation, structure, and hierarchy in multiadaptive games, *Physical Review E* 84 (2011) 061148.
- [56] P. Lozano, S. Gavrillets, A. Sánchez, Cooperation, social norm internalization, and hierarchical societies, *Scientific Reports* 10 (2020) 15359.